

Please cite the Published Version

Palanisamy, S, Ramaraj, SK, Chen, S-M, Velusamy, V, Chiu, T-W, Yang, CK, Chen, T-W and Selvam, S (2017) One pot electrochemical synthesis of poly(melamine) entrapped gold nanoparticles composite for sensitive and low level detection of catechol. Journal of Colloid and Interface Science, 496. pp. 364-370. ISSN 0021-9797

DOI: <https://doi.org/10.1016/j.jcis.2016.12.062>

Publisher: Elsevier

Version: Accepted Version

Downloaded from: <https://e-space.mmu.ac.uk/619512/>

Usage rights:



[Creative Commons: Attribution-Noncommercial-No Derivative Works 4.0](#)

Additional Information: This is an Author Accepted Manuscript of a paper accepted for publication in Journal of Colloid and Interface Science, published by and copyright Elsevier.

Enquiries:

If you have questions about this document, contact openresearch@mmu.ac.uk. Please include the URL of the record in e-space. If you believe that your, or a third party's rights have been compromised through this document please see our Take Down policy (available from <https://www.mmu.ac.uk/library/using-the-library/policies-and-guidelines>)

One pot electrochemical synthesis of poly(melamine) entrapped gold nanoparticles composite for sensitive and low level detection of catechol

Selvakumar Palanisamy¹, Sayee Kannan Ramaraj², Shen-Ming Chen^{*1}, Te-Wei Chiu^{2**},
Vijayalakshmi Velusamy^{3***}

¹Electroanalysis and Bioelectrochemistry Lab, Department of Chemical Engineering and Biotechnology, National Taipei University of Technology, No.1, Section 3, Chung-Hsiao East Road, Taipei 106, Taiwan (R.O.C).

²Department of Materials and Mineral Resources Engineering, National Taipei University of Technology, 1, Sec. 3, Zhongxiao E. Rd., Taipei 106, Taiwan.

³Division of Electrical and Electronic Engineering, School of Engineering, Manchester Metropolitan University, Manchester – M1 5GD, United Kingdom.

Corresponding authors:

S.M. Chen (smchen78@ms15.hinet.net)

T.W. Chiu (tewei@ntut.edu.tw)

V. Velusamy (V.Velusamy@mmu.ac.uk)

Abstract

A simple and cost effective synthesis of nanomaterials with advanced physical and chemical properties have received much attention to the researchers, and is of interest to the researchers from different disciplines. In the present work, we report a simple and one pot electrochemical synthesis of poly(melamine) entrapped gold nanoparticles (PM-AuNPs) composite. The PM-AuNPs composite was prepared by single step electrochemical method, wherein the AuNPs and PM were simultaneously fabricated on the electrode surface. The as-prepared materials were characterized by various physicochemical methods. The PM-AuNPs composite modified electrode was used as an electrocatalyst for oxidation of catechol (CC) due to its well-defined redox behaviour and enhanced electro-oxidation ability towards CC than other modified electrodes. Under optimized conditions, the differential pulse voltammetry (DPV) was used for the determination of CC. The DPV response of CC was linear over the concentration ranging from 0.5 to 175.5 μM with a detection limit of 0.011 μM . The PM-AuNPs composite modified electrode exhibits the high selectivity in the presence of range of potentially interfering compounds including dihydroxybenzene isomers. The sensor shows excellent practicality in CC containing water samples, which reveals the potential ability of PM-AuNPs composite modified electrode towards the determination of CC in real samples.

Keywords: Poly(melamine); gold nanoparticles; electrochemical preparation; catechol; differential pulse voltammetry

1. Introduction

Recent years, the monitoring of phenols and its analogous compounds has received greater attention due to their prime toxicity to animals, plants and aquatic organisms [1]. In particular, catechol (CC) is an isomer of dihydroxybenzene, has poor degradability in water and the large amount has released into the fresh water from the pesticides, dyes and pharmaceutical industries [2]. The U.S Environmental Protection (EPA) Agency and the European Union (EU) has stated that CC as a serious environmental pollutant due to its poor degradability and high toxicity in the biological environment [3, 4]. Hence, the development of reliable and robust methods for the detection of trace levels of CC is more important. To date, number of analytical methodologies have been developed and used for the reliable detection of CC including electrochemical methods [5–9]. Compared with available methods, electrochemical methods are widely used for the detection of CC due to its simplicity, portability and high sensitivity [10]. It is well-known that CC is highly electroactive on conventional carbon electrodes such as glassy and screen printed carbon electrodes, though the selectivity and reproducibility of the electrode is quite challenging due to the fouling of oxidation signals, higher oxidation working potential and response to other compounds [3]. Hence, the different approaches or modifiers have been used on the electrode surfaces to attain the better selectivity and improved sensitivity for the detection of CC.

Recent years, different nano and micro material modified electrodes have been employed for the reliable detection of CC, and they can also offer better selectivity, lower oxidation potential with improved sensitivity [11–15]. For instance, carbon nanomaterials and metal nanoparticles are widely used for selective detection of CC due to their unique physical and chemical properties [3, 11–17]. Among them, metal nanoparticles are found considerable interest

in the modified electrodes owing to the large active sites and high conductivity [18]. In particular, Au-NPs are commonly used for broad range of applications including the electrochemical sensing of small molecules [3]. On the other hand, poly(melamine) (PM) is an important polymer, has been widely used for the construction of electrochemical sensors due to its extreme stability and presence of abundant nitrogen functional groups [19–23]. The abundant functional groups and extreme hydrophilicity of PM is often more helpful for the surface functionalization with small molecules. Up to now, very few reports have been reported for the synthesis of PM with metal nanoparticles, while they not yet been used for electrochemical sensor applications.

The motivation of the present work is to synthesize the AuNPs-PM composite by single step electrochemical method for the first time. The schematic representation for the single step electrochemical fabrication of PM-AuNPs composite is shown in **Fig. 1**. The resulting AuNPs-PM composite is used for the sensitive and low potential detection of CC. The combined unique properties of AuNPs and PM are result into the high sensitivity, selectivity and lower oxidation potential for CC than discrete PM and AuNPs modified electrodes.

2. Experimental

2.1. Materials and methods

Melamine was obtained from Sigma–Aldrich and used as received. Potassium gold (III) chloride trihydrate ($\text{KAuCl}_4 \cdot 3\text{H}_2\text{O}$) was purchased from Strem chemicals (USA). Catechol was purchased from Sigma–Aldrich. NaH_2PO_4 and Na_2HPO_4 were purchased from Sigma–Aldrich and Avantor Performance Materials Inc, Center Valley, U.S.A, respectively. The phosphate buffer solution (PBS) pH 7.0 was prepared using 0.05 mol L^{-1} Na_2HPO_4 and NaH_2PO_4 solutions in double distilled water. All other chemical were used in this study were obtained from Aldrich and the solutions were prepared using doubly distilled water without any further purification.

Cyclic voltammetry (CV) and differential pulse voltammetry (DPV) experiments were performed using a computerized CHI 1205b and CHI750a electrochemical work stations. The scanning electron microscopic (SEM) images were acquired using Hitachi S-3000 H electron microscope. Transmission electron microscopic image of the composite was taken using JEM 2007 model transmission electron microscope (TEM). Elemental analysis (EDS) of the composite was analyzed using HORIBA EMAX X-ACT attached Hitachi S-3000 H scanning electron microscope. Thermo SCIENTIFIC Nicolet iS10 instrument was used for the Fourier transform infrared spectroscopy (FT-IR) measurements. Typical three electrode setup which consisting of glassy carbon electrode as a working electrode, a saturated Ag/AgCl reference electrode and a platinum electrode as an auxiliary electrode in the electrochemical experiments. All measurements were carried out at a room temperature in an inert atmosphere unless otherwise stated.

2.2. single step electrochemical synthesis of PM-AuNPs composite

To prepare PM–AuNPs composite, first 1 mM $\text{KAuCl}_4 \cdot 3\text{H}_2\text{O}$ solution was prepared using 0.5 M H_2SO_4 and melamine (1 mM) was added into the solution and sonicated for 10 min. The pre-cleaned GCE was immersed in the electrochemical cell containing 1 mM melamine, 1 mM $\text{KAuCl}_4 \cdot 3\text{H}_2\text{O}$ and 0.5 M H_2SO_4 and performed the CV for 10 constitutive cycles in the potential ranging from 0 to 1.5 V at a scan rate of 50 mV/s [18], as shown in **Fig. 1**. After the constitutive CV cycles, the PM-AuNPs composite was fabricated on the electrode surface, and resulting electrode gently rinsed with water and dried in an air oven. The AuNPs and PM modified electrodes were prepared by similar method without melamine and $\text{KAuCl}_4 \cdot 3\text{H}_2\text{O}$. All electrodes were stored under dry conditions when not in use. The electrochemical measurements were performed in the presence of high purity nitrogen gas.

3. Results and discussion

3.1. Characterizations

The physicochemical properties of the as-prepared materials were characterized by SEM, TEM and FTIR spectroscopy. **Fig. 2** shows the SEM images of AuNPs (A) and PM-AuNPs composite (B). The TEM image of PM-AuNPs composite is shown in **Fig. 2C**. The SEM image of electrodeposited AuNPs shows that the aggregated spherical nanoparticles with an average diameter about 72 nm. The SEM image of PM-AuNPs shows the uniform distribution of AuNPs with the diameter of 70 nm, where the AuNPs were covered by a thin layer of PM. The TEM image of PM-AuNPs confirms that the spherical AuNPs were covered by PM thin layer. It is noted that the PM layer was interlinked with each AuNPs and the average size of AuNPs was found as 70 nm, which is in good agreement with SEM image of PM-AuNPs composite. The strong interactions between the AuNPs and PM are result into the formation of PM-AuNPs composite, and the structure of PM-AuNPs composite is shown in **Fig. 1**. The presence of AUNPs in PM-AuNPs was confirmed by elemental analysis (EDS) and shown in **Fig. 2D**. The EDS result confirms the presence of metallic Au in PM-AuNPs composite, which supports the formation of PM-AuNPs composite.

The FTIR was further used to investigate the formation of PM-AuNPs composite, and the corresponding FTIR spectra of melamine and PM-AuNPs is shown in **Fig. 3**. The FTIR spectrum of melamine (black line) shows three distinct bands at 3466, 3258, and 3122 cm^{-1} are characteristic peaks for N–H (asymmetric), and N–H (symmetric) stretching vibrations of melamine [24]. In addition, two new band were observed at 1683 and 1580 cm^{-1} are due to the characteristic amine II and III bonds of melamine [24]. However, the bands related to–NH stretching vibrations at 3280–3500 cm^{-1} are absent in PM–AuNPs composite (red line), which

revealed the polymerization of melamine on AuNPs surface. The result confirms the formation of PM-AuNPs composite.

3.2. Electrochemical behavior of CC

To investigate the electrochemical behavior of CC, the different modified electrodes were investigated by cyclic voltammetry in the presence of 25 μ M CC in PBS at a scan rate of 50 mV/s. The comparative cyclic voltammetric results are shown in **Fig. 4**. It can be seen that the bare electrode (blue curve) did not show any apparent signal for CC, which indicates that the bare electrode has poor electrochemical activity towards CC. The PM modified electrode (light green) shows a well-defined quasi-reversible redox couple for CC, and the oxidation and reduction peaks were appeared at 0.266 and 0.172 V, respectively. The redox behavior is due to the reversible oxidation of CC to corresponding quinone derivative [3]. The AuNPs modified electrode (dark green) shows an enhanced quasi-redox couple for CC, and the anodic and cathodic peak potential were appeared at 0.232 and 0.186 V, respectively. In addition, the observed oxidation peak current of CC was higher than PM modified electrode. On the other hand, an enhanced and well-defined reversible redox couple of CC was observed at PM-AuNPs modified electrode (red curve). The oxidation and reduction peak of CC was appeared at 0.116 and 0.216 V, respectively. The observed oxidation peak current of CC was 4 folds higher than those observed at PM and AuNPs modified electrodes, which indicates that the PM-AuNPs modified electrode has high electrochemical activity towards CC than other modified electrodes. The enhanced electrochemical behavior of CC is due to the combined unique properties of PM and AuNPs. The AuNPs is provided more active sites and PM provides a suitable matrix for adsorption of more CC molecules. In addition, the composite more likely acted as an accelerator of the electron transfer between CC and the electrode and result into the enhanced and well-

defined redox behavior of CC. **Fig. 5A** shows the typical cyclic voltammetry response of PM-AuNPs modified electrode in PBS containing 20 μM CC at different sweeping scan rates; the scan rates were tested from 20 to 200 mV/s. It can be clearly seen that the anodic and cathodic peak current of CC increases with the increasing the scan rates, and corresponding peak currents of CC have a linear dependence with the square root of scan rates from 20 to 200 mV/s (**Fig. 5A inset**). The linear regression equations for anodic and cathodic peak currents were expressed as: $I_{pa} (\mu\text{A}) = 1.2823 - 1.3334 \sqrt{v/\text{mV/s}}$ ($R^2 = 0.9989$) and $I_{pc} (\mu\text{A}) = -1.1537 - 0.0301 \sqrt{v/\text{mV/s}}$ ($R^2 = 0.9993$). The result indicates that the electrochemical behavior of CC at PM-AuNPs modified electrode is a typical diffusion-controlled electrochemical process [3].

We have also studied the effect of pH on the electrochemical behavior of CC by cyclic voltammetry. **Fig. 5B** depicts the cyclic voltammetry response of PM-AuNPs modified electrode in 20 μM CC containing different pH (pH 3, 5, 7, 9 and 11) and the scan rate was 50 mV/s. The anodic and cathodic peak potential of CC shifted towards negative direction upon increasing the pH from 3 to 11 and shifts towards positive direction upon decreasing the pH from 11 to 3. The result indicates that the protons are involved in the redox behavior of CC. We have also made the plot for the formal potential ($E^{0'}$) vs. pH and the $E^{0'}$ was linear dependence with the pH from 3 to 11 (**Fig. 5B inset**). The slope and correlation coefficient was found as -58.4 mV/pH and 0.9969, respectively. The obtained slope value of CC (-58.4 mV/pH) is very close to the Nernstian equation theoretical value (-59.6 mV/pH) of an equal number of protons and electrons transferred electrochemical redox process [3]. The electrochemical redox process of CC at PM-AuNPs modified electrode is shown in **Fig. 6**.

3.3. Determination of CC

Under optimized conditions, the DPV was used for the electrochemical determination of CC using PM-AuNPs modified electrode, due to its high sensitivity than other voltammetric methods. **Fig. 7** shows the typical DPV response of PM-AuNPs modified electrode for addition of different concentrations of CC (0.5–196.5 μM) into the PBS. It can be clearly seen that a noteworthy DPV response was observed for the addition of 0.5, 1 and 3 μM CC (first three additions) into the PBS, and the response current increases with increasing the concentrations of CC. As shown in **Fig. 7 inset**, the DPV response of PM-AuNPs modified electrode was proportional to the concentration of CC in the linear response ranging from 0.5 to 175.5 μM . The linear regression equation was found as $I_{\text{pa}} (\mu\text{A}) = 0.1156 + 0.9831 C/\mu\text{M}$ ($R^2 = 0.9878$). The limit of detection (LOD) was calculated as 0.011 μM based on IUPAC recommendations ($S/N=3$). The sensor sensitivity was calculated as $2.15 \mu\text{A}\mu\text{M}^{-1} \text{ cm}^{-2}$ using slope/electrochemically active surface area of the electrode, where the electrochemically active surface area of the electrode is 0.167 cm^2 and was calculated using Randles–Sevcik equation. To verify the novelty and analytical advantages of the as-prepared sensor, the obtained analytical results are compared with previously reported CC sensors. The PM-AuNPs modified electrode exhibited a lower LOD for the determination of CC than previously reported CC sensors [2–4, 10–12, 15–17, 20, 25, 26]. For instance, the LOD of sensor (0.011 μM) was lower than previously reported graphene–chitosan [2] (0.75 μM), gold nanoparticles/graphene oxide@polydopamine [3] (0.015 μM), CdSe nanosheets [4] (0.6 μM), carbon/ionic liquids [10] (0.6 μM), graphene/lanthanum hydroxide nanowires [11] (0.1 μM), carbon nano-fragment [12] (0.1 μM), carbon nanotubes-ionic liquid [15] (0.6 μM), reduced graphene oxide [16] (0.1 μM), reduced graphene oxide/copper nanoparticles [17] (0.025 μM), poly(melamine)/electrochemically reduced graphene oxide/Cu nanoparticles [20] (0.15 μM), graphene–TiO₂ [25] (0.087 μM) and

carbon nanocages-reduced graphene oxide [26] (0.4 μM) modified electrodes for the detection of CC. In addition, the linear response range and sensitivity of the as-prepared sensor was comparable with aforementioned CC sensors. Hence, the PM-AuNPs composite can be used as a promising electrode material for sensitive and low level determination of CC.

3.4. Selectivity studies

The selectivity of the sensor is more important especially the electrode working in positive potentials, since the range of compounds can be easily oxidized at positive working potentials such as dopamine (DA), uric acid (UA), ascorbic acid (AA), hydroquinone (HQ) and epinephrine (EP). Hence, we have evaluated the selectivity of sensor by DPV in the presence of CC with dopamine, uric acid, ascorbic acid, hydroquinone and epinephrine. **Fig. 8** shows the DPV response of PM-AuNPs composite modified electrode for the addition of 1 μM CC with 100 μM concentration additions of DA, UA, AA, HQ and EP into the PBS. It can be seen that the DPV response of CC was unchanged, and had no effect on the electrode surface. In addition, the oxidation peak potential of CC was not affected by the interfering species, which indicates the high selectivity of the PM-AuNPs composite modified electrode towards CC. However, 100 μM addition of HQ showed a little response on the electrode surface due to its similar structural and chemical properties to CC. The result confirms that PM-AuNPs composite modified electrode can be used for selective detection of CC.

3.5. Determination of CC in water samples

The real time application of the sensor is more important in order to use the electrode in environmental samples. Hence, the practicality of the PM-AuNPs composite modified electrode was evaluated towards the determination of CC in different water samples. We have chosen the tap and drinking water samples for real sample analysis due to the less complexity. The DPV

was used for the detection of CC in water samples and the recoveries were calculated using the standard addition method [3]. All the experimental conditions are similar to **Fig. 7**. The obtained recoveries of CC in tap and drinking water samples are summarized in **Table 1**. It can be seen that the average recoveries of CC were 97.5% in tap water and 97.2% in drinking water samples with an appropriate relative standard deviation (RSD). The result confirms that PM-AuNPs composite modified electrode can be used for accurate determination of CC in environmental real samples.

Under the optimum conditions, the reproducibility and repeatability of the PM-AuNPs composite modified electrode was evaluated in the PBS containing 20 μM CC by cyclic voltammetry (not shown). The experimental working conditions are similar to **Fig. 4**. The PM-AuNPs composite modified electrode regenerated its oxidation peak current with RSD of 1.6% using five different sensors. Appropriate repeatability was observed with RSD of 2.1% for single PM-AuNPs composite modified electrode for 10 continues measurements. The results revealed that the PM-AuNPs composite modified electrode has good reproducibility and repeatability. The storage stability of the PM-AuNPs composite modified electrode towards detection of 20 μM CC was monitored periodically by CV (not shown). The PM-AuNPs composite modified electrode retains 96.8% of its original sensor response (oxidation peak current) to CC after two-weeks storage in PBS. The result indicates the high storage stability of the PM-AuNPs composite modified electrode towards CC.

4. Conclusions

In conclusion, we have prepared PM-AuNPs composite modified electrode by single step electrochemical method for the first time. The PM-AuNPs composite modified electrode was used for a simple and robust electrochemical sensor for the detection of CC, which is based on its

electrocatalytic activity towards CC. The developed sensor exhibited a lower LOD (11 nM), appropriate linear response ranges (up to 175.5 μM) and high sensitivity ($2.15 \mu\text{A}\mu\text{M}^{-1} \text{cm}^{-2}$) for the determination of CC. The PM-AuNPs composite modified electrode showed satisfactory recovery of CC in water samples, which authenticates its practical capability towards the detection of CC in real samples. The sensor also showed high selectivity towards CC in the presence of range of potentially interfering compounds including 100-fold presence of HQ. As a future perspective, the PM-AuNPs composite can be used as a viable material for selective and precise determination of trace levels of CC in environmental samples. In addition, PM-AuNPs composite can be used for developing new sensor devices in the near future.

Acknowledgments

This project was supported by the Ministry of Science and Technology, (project no. NSC1012113M027001MY3), Taiwan (Republic of China).

Competing financial interests

The authors declare no competing financial interests.

References

- [1] N.M. Vad, P.K. Kandala, S.K. Srivastava, M.Y. Moridani, Structure–toxicity relationship of phenolic analogs as anti-melanoma agents: An enzyme directed prodrug approach, *Chem. Biol. Interact.* 183 (2010) 462–471.
- [2] H.S. Yin, Q.M. Zhang, Y.L. Zhou, Q. Ma, Electrochemical behavior of catechol, resorcinol and hydroquinone at graphene–chitosan composite film modified glassy carbon electrode and their simultaneous determination in water samples, *Electrochim. Acta*, 56 (2011) 2748–2753.
- [3] S. Palanisamy, K. Thangavelu, S.M. Chen, B. Thirumalraj, X.H. Liu, Preparation and characterization of gold nanoparticles decorated on graphene oxide@ polydopamine composite: Application for sensitive and low potential detection of catechol, *Sens. Actuators B*, 233 (2016) 298–306.
- [4] X. Cao, X. Cai, Q. Feng, S. Jia, N. Wang, Ultrathin CdSe nanosheets: synthesis and application in simultaneous determination of catechol and hydroquinone, *Anal. Chim. Acta*, 752 (2012) 101–105.
- [5] G. Marrubini, E. Calleri, T. Coccini, A. Castoldi, L. Manzo, Direct analysis of phenol, catechol and hydroquinone in human urine by coupled-column HPLC with fluorimetric detection, *Chromatographia*, 62 (2005) 25–31.
- [6] M.F. Pistonesi, M.S.D. Nezio, M.E. Centurión, M.E. Palomeque, A.G. Lista, B.S. Fernández, Band Determination of phenol, resorcinol and hydroquinone in air samples by synchronous fluorescence using partial least-squares (PLS), *Talanta*, 69 (2006) 1265–1268.
- [7] Afkhami, H.A. Khatami, Indirect kinetic–spectrophotometric determination of resorcinol, catechol, and hydroquinone, *J. Anal. Chem.*, 56 (2001) 429–432.
- [8] L.J. Zhao, B.Q. Lu, H.Y. Yuan, Z.D. Zhou, D. Xiao, A sensitive chemiluminescence method for determination of hydroquinone and catechol, *Sensors*, 7 (2007) 578–588.

- [9] N. Abdellatif, P. Cañizares, C. Sáez, J. Lobato, M.A. Rodrigo, Electrochemical oxidation of hydroquinone, resorcinol, and catechol on boron-doped diamond anodes, *Environ. Sci. Technol.*, 39 (2005) 7234–7239.
- [10] Z. Hong, L. Zhou, J. Li, J. Tang, A sensor based on graphitic mesoporous carbon/ionic liquids composite film for simultaneous determination of hydroquinone and catechol, *Electrochim. Acta*, 109 (2013) 671–677.
- [11] Z. Guo, Y. Lu, J. Li, X. Xu, G. Huang, Z. Wang, Simultaneous determination of hydroquinone and catechol using electrode modified by composite of graphene/lanthanum hydroxide nanowires, *Anal. Methods*, 6 (2014) 8314–8320.
- [12] C. Zhang, L. Zeng, X. Zhu, C. Yu, X. Zuo, X. Xiao, J. Nan, Electrocatalytic oxidation and simultaneous determination of catechol and hydroquinone at a novel carbon nano-fragment modified glassy carbon electrode, *Anal. Methods*, 5 (2013) 2203–2208.
- [13] Y. Yang, Q. Wang, W. Qiu, H. Guo, F. Gao, Covalent immobilization of $\text{Cu}_3(\text{btc})_2$ at chitosan–electroreduced graphene oxide hybrid film and its application for simultaneous detection of dihydroxybenzene isomers, *J. Phys. Chem. C*, 120 (2016) 9794–9803.
- [14] Y. Wang, S. Hu, Applications of carbon nanotubes and graphene for electrochemical sensing of environmental pollutants, *J. Nanosci. Nanotechnol.* 16 (2016) 7852–7872.
- [15] C. Bu, X. Liu, Y. Zhang, L. Li, X. Zhou, X. Lu, A sensor based on the carbon nanotubes-ionic liquid composite for simultaneous determination of hydroquinone and catechol, *Colloids Surf. B*, 88 (2011) 292–296.
- [16] L.Y. Chen, Y.H. Tang, K. Wang, C.B. Liu, Direct electrodeposition of reduced graphene oxide on glassy carbon electrode and its electrochemical application, *Electrochem. Commun.* 13 (2011) 133–137.

- [17] S. Palanisamy, C. Karuppiyah, S.M. Chen, C.Y. Yang, P. Periakaruppan, Simultaneous and selective electrochemical determination of dihydroxybenzene isomers at a reduced graphene oxide and copper nanoparticles composite modified glassy carbon electrode, *Anal. Methods*, 6 (2014) 4271-4278.
- [18] C. Karuppiyah, S. Palanisamy, S.M. Chen, S.K. Ramaraj, P. Periakaruppan, A novel and sensitive amperometric hydrazine sensor based on gold nanoparticles decorated graphite nanosheets modified screen printed carbon electrode, *Electrochim. Acta*, 139 (2014) 157-164.
- [19] S. He, Z. Chen, Y. Yu, L. Shi, A novel non-enzymatic hydrogen peroxide sensor based on poly-melamine film modified with platinum nanoparticles, *RSC Adv.* 4 (2014) 45185–45190.
- [20] P.S. Dorraji, F.A. Jalaliz, nanocomposite of poly(melamine) and electrochemically reduced graphene oxide decorated with Cu nanoparticles: Application to simultaneous determination of hydroquinone and catechol, *J. Electrochem. Soc.* 162 (2015) B237-B244.
- [21] Y.L. Su, S.H. Cheng, Sensitive and selective determination of gallic acid in green tea samples based on an electrochemical platform of poly(melamine) film, *Anal Chim. Acta*, 901 (2015) 41–50.
- [22] J. Peng, Y. Feng, X. Han, Z.N. Gao, Simultaneous determination of bisphenol A and hydroquinone using a poly(melamine) coated graphene doped carbon paste electrode, *Microchim. Acta*. 183 (2016) 2289–2296.
- [23] X. Liu, L. Luo, Y. Ding, Q. Wu, Y. Wei, D. Ye, A highly sensitive method for determination of guanine, adenine and epinephrine using poly-melamine film modified glassy carbon electrode, *J. Electroanal. Chem.* 675 (2012) 47–53.

- [24] Z. Chen, J. Wang, F. Yu, Z. Zhang, X. Gao, Preparation and properties of graphene oxide-modified poly(melamine-formaldehyde) microcapsules containing phase change material n-dodecanol for thermal energy storage, *J. Mater. Chem. A*, 3 (2015) 11624–11630.
- [25] Y. Zhang, S. Xiao, J. Xie, Z. Yang, P. Pang, Y. Gao, Simultaneous electrochemical determination of catechol and hydroquinone based on graphene–TiO₂ nanocomposite modified glassy carbon electrode, *Sensors and Actuators B*, 204 (2014) 102–108.
- [26] Y.H. Huang, J.H. Chen, X. Sun, Z.B. Su, H.T. Xing, S.R. Hu, W. Weng, H.X. Guo, W.B. Wu, Y.S. He, One-pot hydrothermal synthesis carbon nanocages-reduced graphene oxide composites for simultaneous electrochemical detection of catechol and hydroquinone, *Sensors and Actuators B*, 212 (2015) 165–173.

Table 1. Determination of CC in tap and drinking water samples using PM-AuNPs composite modified electrode by DPV. RSD is related to 3 measurements.

Sample	Added (μM)	Found (μM)	Recovery (%)	RSD (%)
Tap water	–	ND	–	–
	2.0	1.94	97.0	1.6
	4.0	3.92	98.0	1.9
Drinking water	–	ND	–	–
	2.0	1.91	95.5	2.9
	4.0	3.95	98.8	2.5

ND – Not detected.

Figure captions

Figure 1. Schematic representation of one pot electrochemical preparation of PM–AuNPs composite.

Figure 2. SEM images of AuNPs (A) and PM–AuNPs composite (B). TEM image of PM–AuNPs composite (C) and the representative EDS of PM–AuNPs composite (D).

Figure 3. FTIR spectra of melamine (black line) and PM-AuNPs composite (red line).

Figure 4. A) Cyclic voltammograms of bare (blue color), PM (light green color), AuNPs (dark green color) and PM-AuNPs (red color) modified electrodes for the response to 20 μM CC in N_2 saturated PBS; Scan rate = 50 mV/s.

Figure 5. A) Cyclic voltammograms obtained at PM-AuNPs composite modified electrode in PBS containing 20 μM CC at different scan rates from 20 to 200 mV/s. B) Cyclic voltammetry response of PM-AuNPs composite modified electrode in 20 μM CC containing different pH (pH 3, 5, 7, 9 and 11) at a scan rate of 50 mV/s. C) Linear plot for the square root of scan rates vs. anodic and cathodic peak current of CC. D) Linear plot for pH vs. formal potential of CC.

Figure 6. Scheme for the electrochemical redox mechanism of CC on PM-AuNPs composite.

Figure 7. DPV response of PM-AuNPs composite modified electrode for different concentration additions of CC (0.5–196.5 μM) into the N_2 saturated PBS. Inset is the calibration plot for current response vs. [CC].

Figure 8. DPV response of PM-AuNPs composite modified electrode for the addition of 1 μM CA with 100 μM concentration additions of AA, DA, UA, EP and HQ into the PBS.

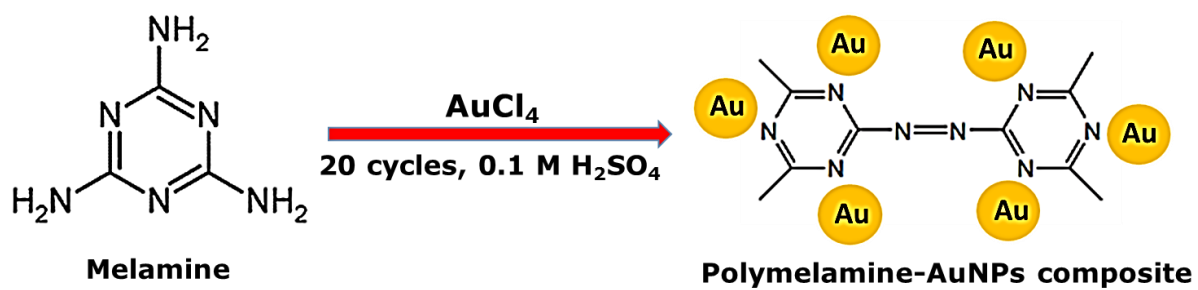


Figure 1

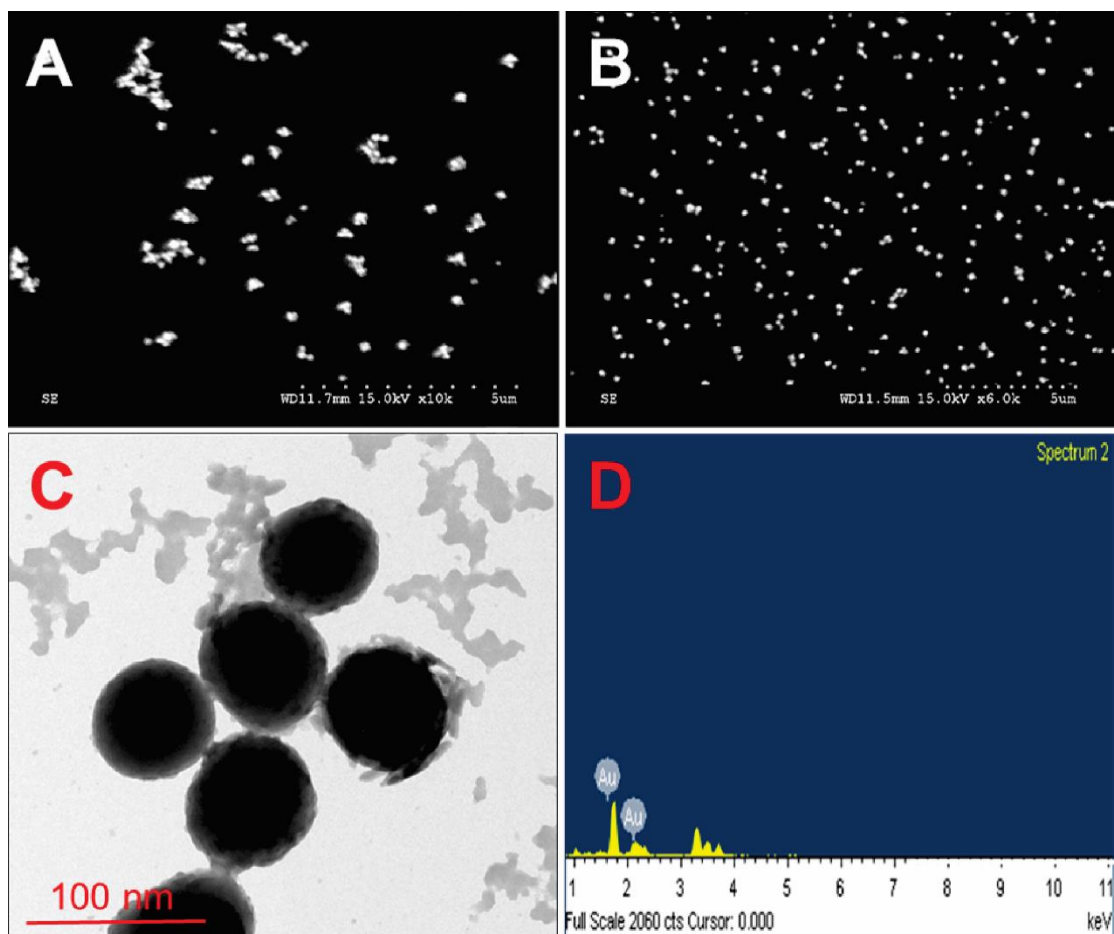


Figure 2

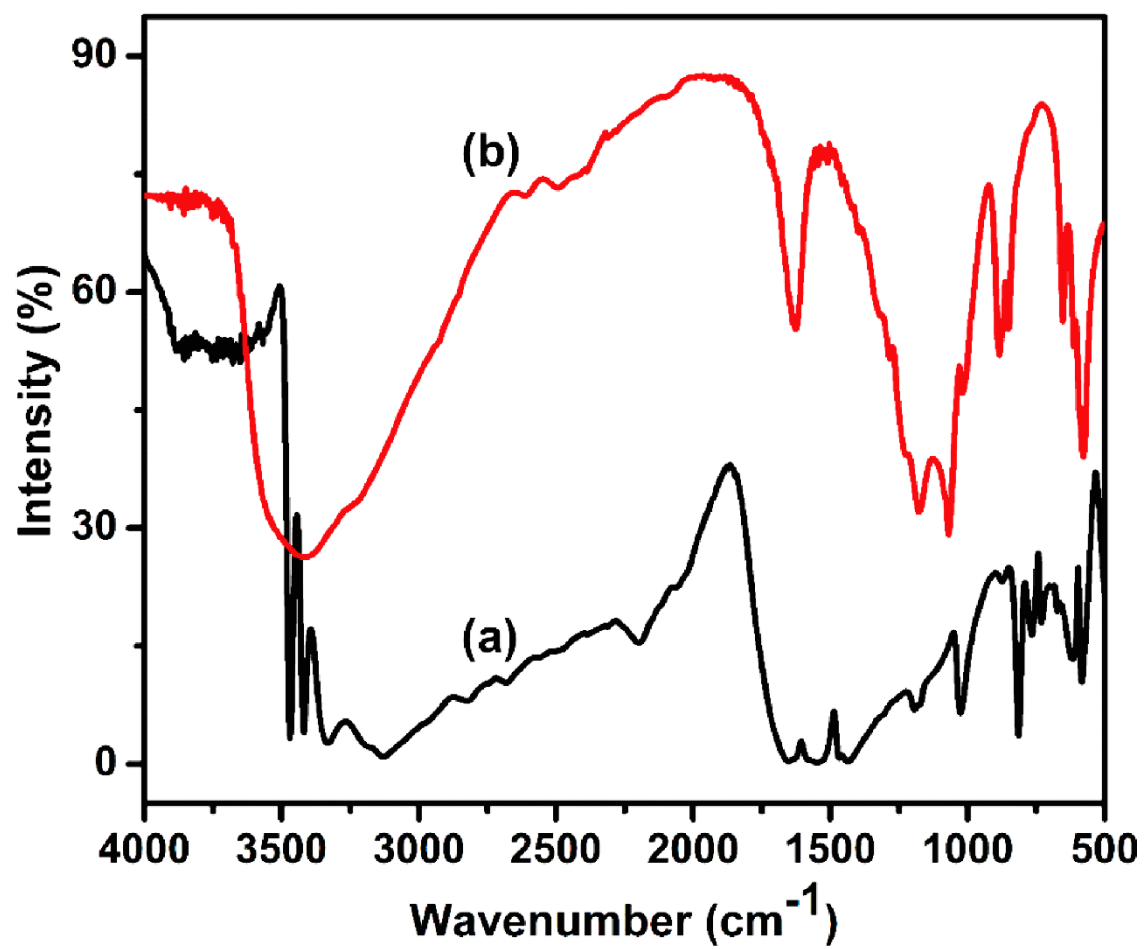


Figure 3

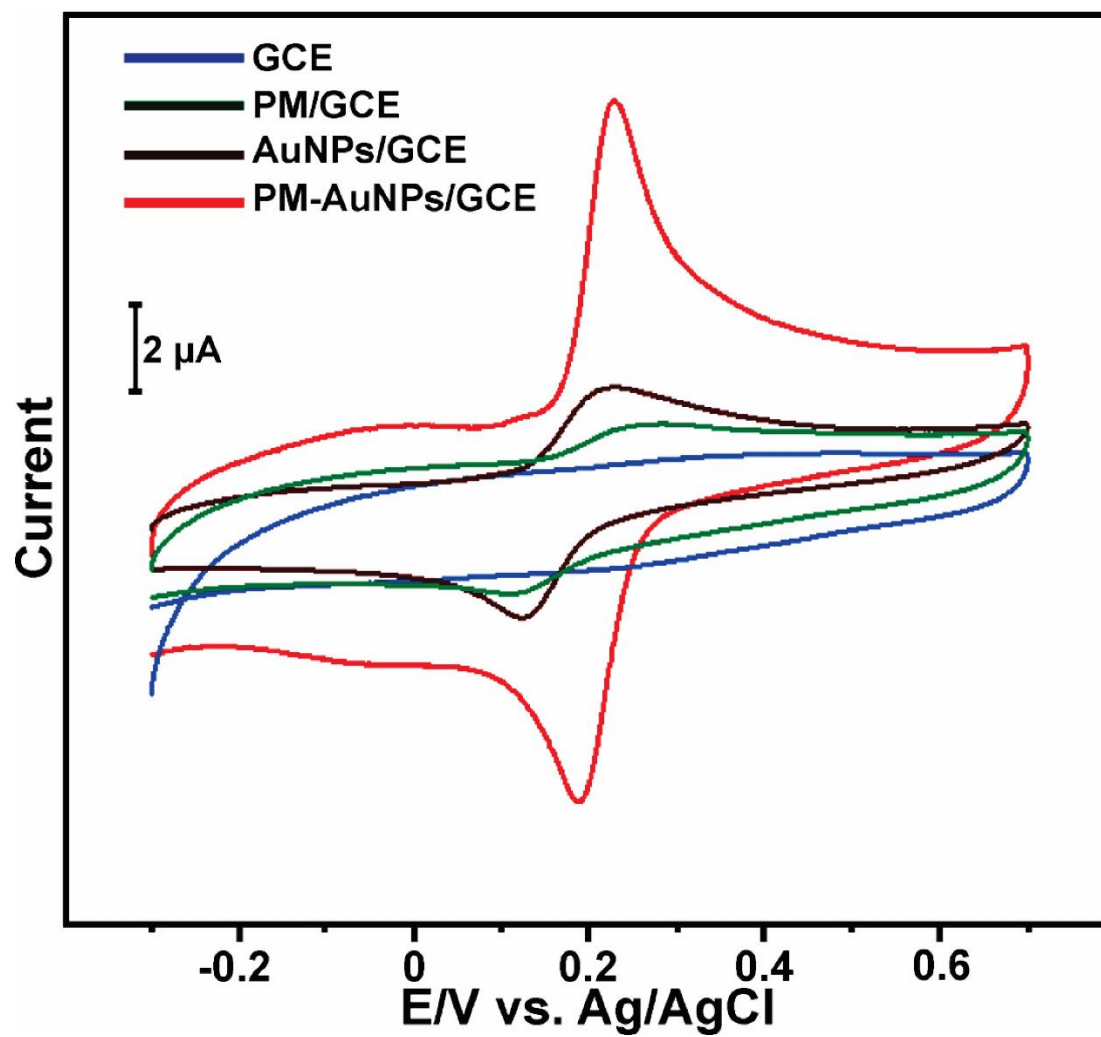


Figure 4

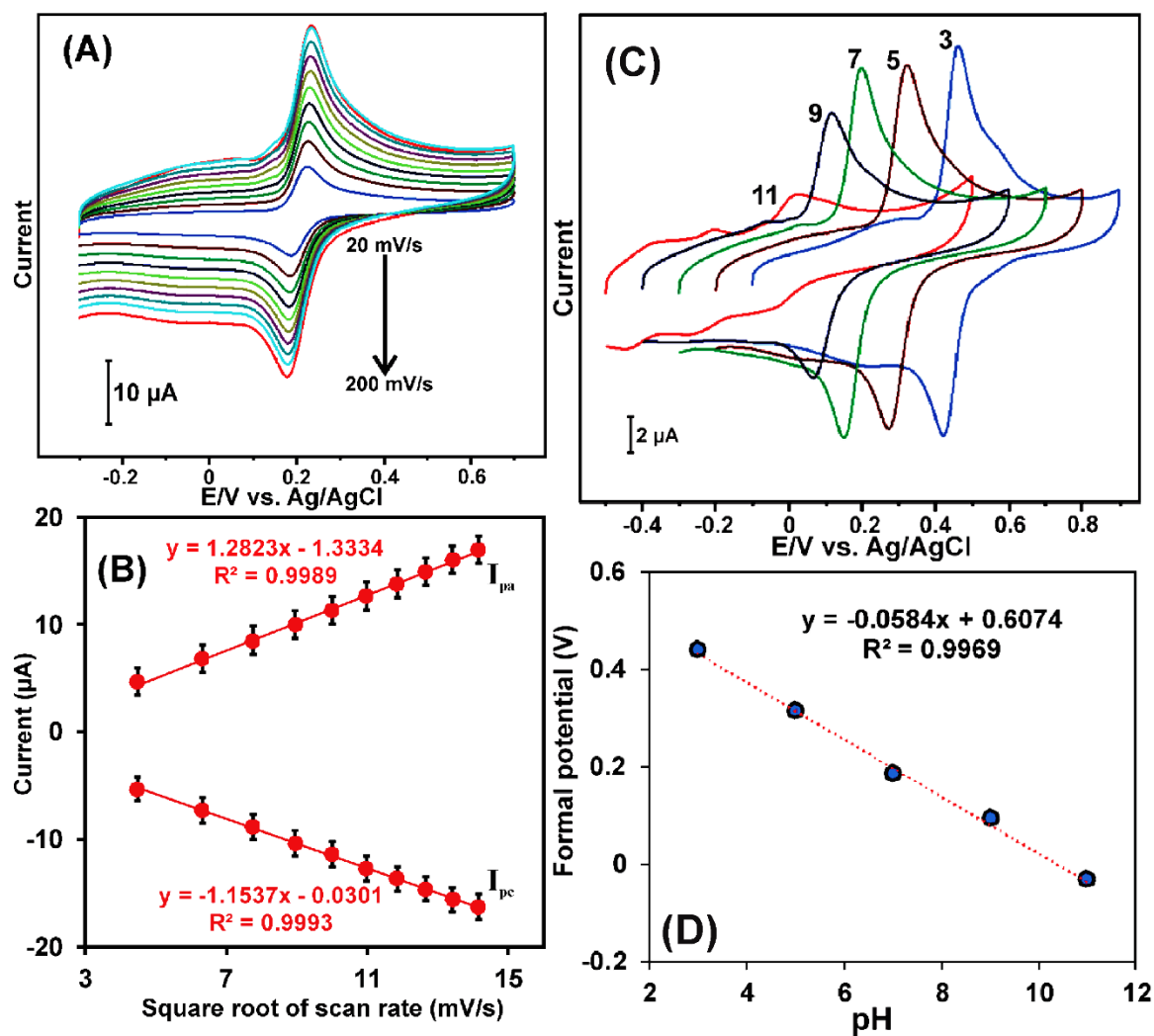


Figure 5

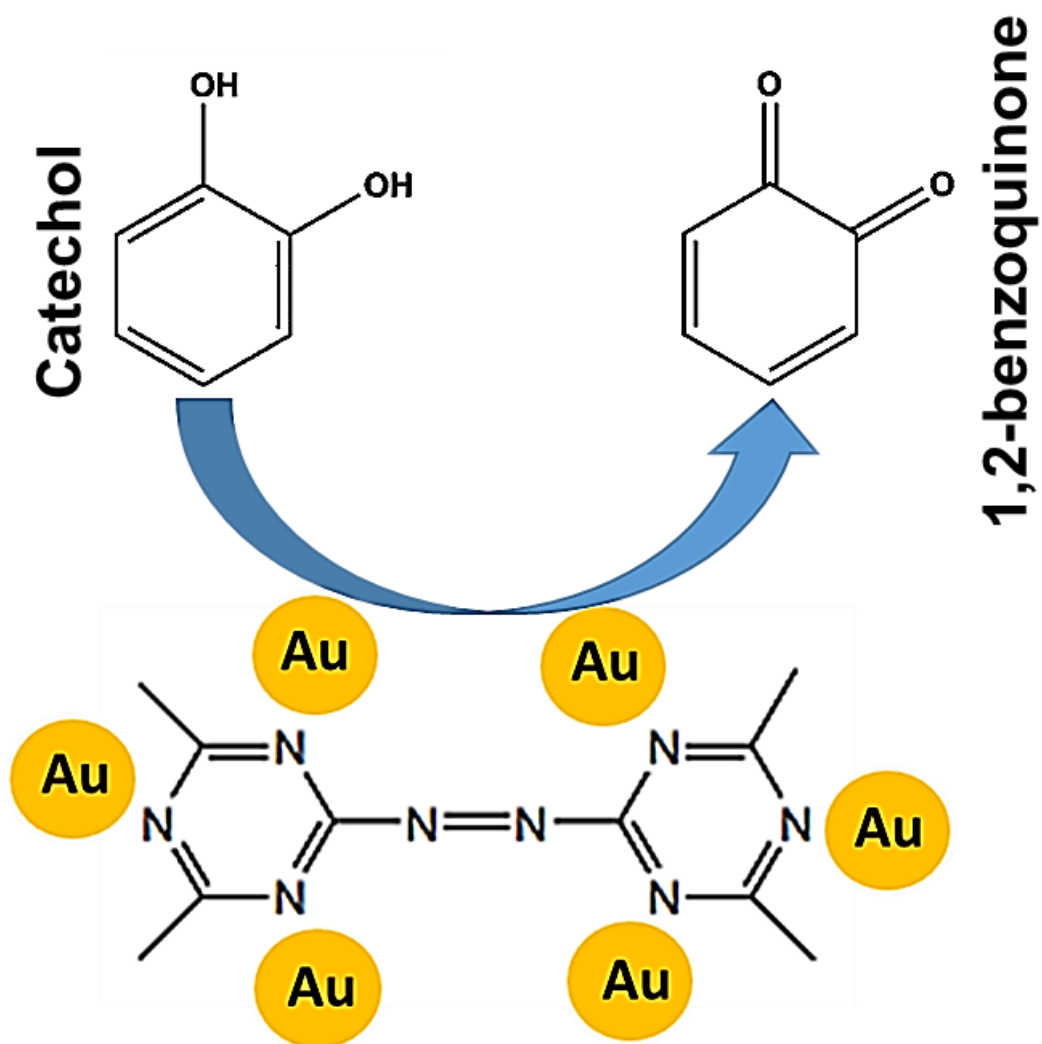


Figure 6

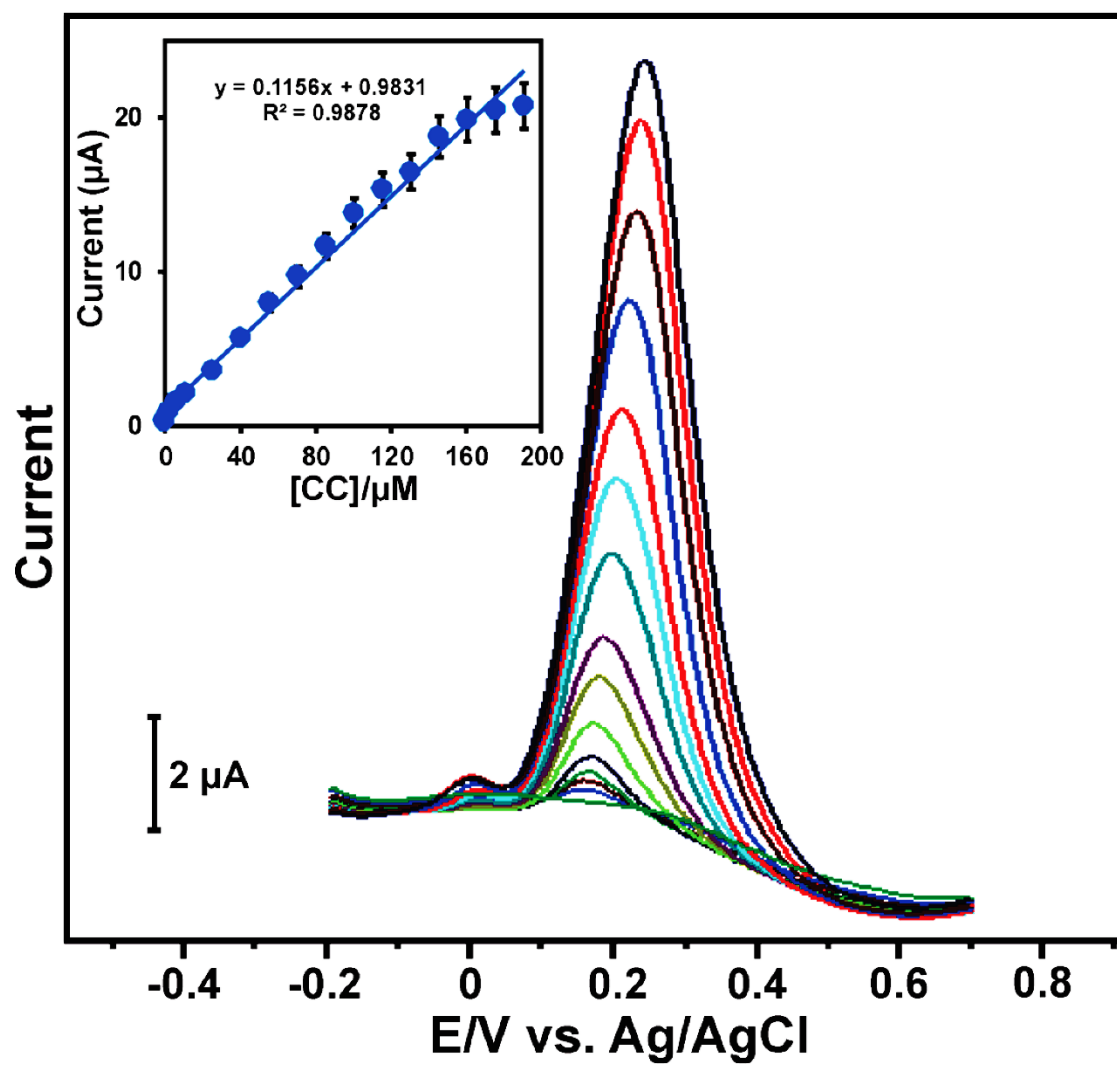


Figure 7

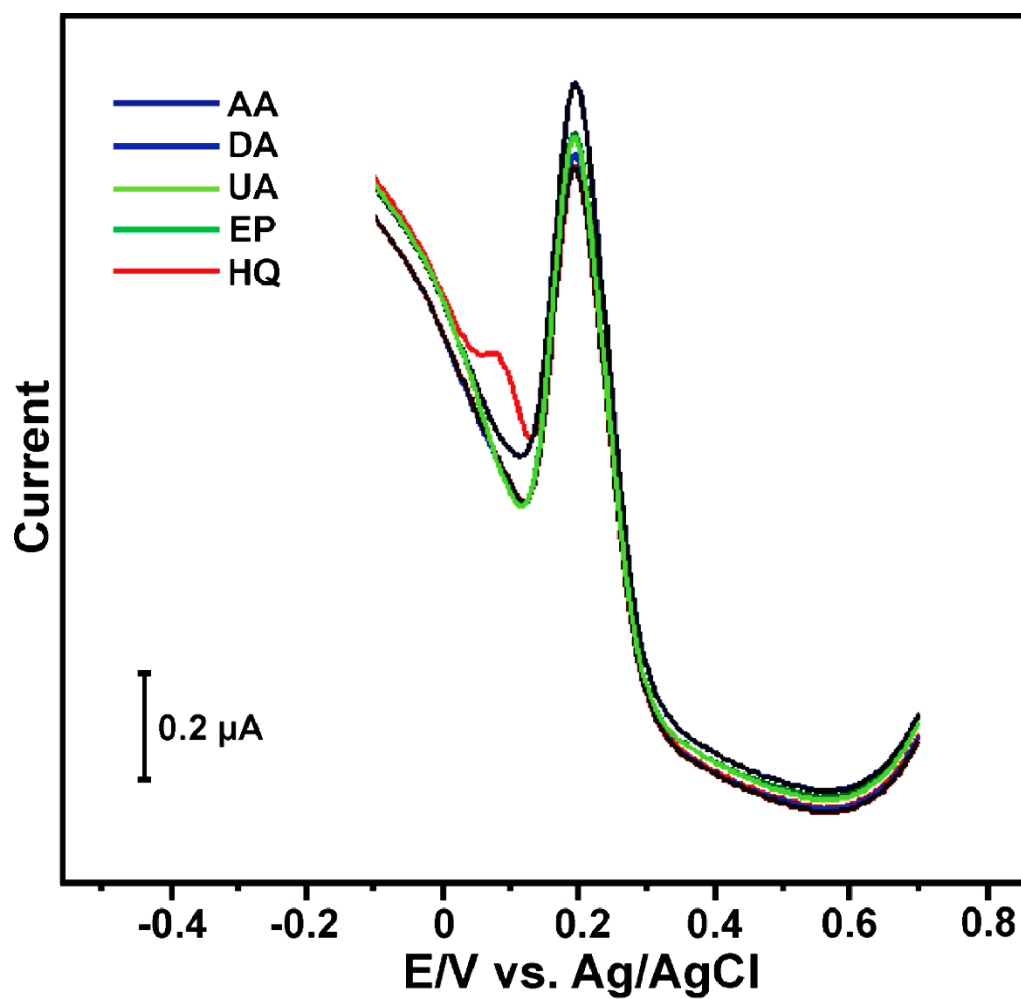


Figure 8